A Length Scale Approach to the Highest Standing Water Wave

Peder A. Tyvand[1] and Jonas Kristiansen Nøland[2]
[1)]*Norwegian University of Life Sciences (NMBU), 1432 Ås, Norway, Tlf.: +47-67231564.*
[2)]*Norwegian University of Science and Technology (NTNU), 7034 Trondheim, Norway, Tlf.: +47-73594202.*

(*Electronic mail: Peder.Tyvand@nmbu.no.)

(Dated: 25 June 2021)

The highest standing surface wave at infinite depth is a classical hydrodynamic problem, illuminated by Taylor's excellent experiments [Taylor, G. I., Proc. R. Soc. Lond. Ser. A 218, 44 (1953)]. Based on length scale arguments, we present a compact analytical approach to the highest standing wave. Our physical postulate is that the highest deep-water wave has a single length scale, i.e., its wavelength. The single-scale postulate for standing periodic deep-water waves is confronted with two distinctly different cases where zero and two length scales are postulated, as follows: (i) No physical length scale for an isolated rogue-wave peak at deep water suggests a similarity solution. (ii) Two length scales for the periodic peaked surface at constant depth suggest a one-parameter family of standing waves. Moreover, the two length scales are the wavelength and average fluid depth. The deep-water limit with its single-length scale postulate confirms Grant's theory [Grant, M. A., J. Fluid Mech. 60, 593 (1973)], taking the highest standing wave as a state of zero kinetic energy. The reversible motion is irrotational according to Lord Kelvin's theorem. The acceleration field for the highest deep-water wave has a single Fourier component according to our single length scale postulate. The resulting free-surface shape follows from the exact nonlinear dynamic condition. Our analytical theory confirms the ratio 0.203 for maximal wave height to wavelength, found by Grant. We test its robustness by extending the theory to a moderate spatial quasi-periodicity. Appendix A provides a simple proof for the right-angle peak, representing a regular extremal point of a locally quadratic complex function. Appendix B presents a quadrupole solution for an isolated peak of stagnant deep-water rogue waves.

I. INTRODUCTION

A classical challenge of hydrodynamics is to determine the maximal wave height of periodic progressive deep-water waves. Stokes[1] pioneered this nonlinear theory and showed that the highest periodic waves have a peak angle of 120°. Already Michell[2] calculated a reasonably accurate value of $H/L = 0.142$ for the ratio of wave height H to wavelength L for these peaked progressive Stokes waves. Modern numerical computations produce the more exact value of $H/L = 0.1412$, see Schwartz & Fenton[3].

In the present paper, we consider the highest standing wave on deep water. This topic is related to but distinctively different from the highest progressive waves. The theory on nonlinear standing waves was initiated by Strutt[5], but he did not describe the highest standing waves. This was first done by Penney & Price[6], who showed that the maximal height of time-periodic standing waves is higher than that of progressive waves. They calculated the value of $H/L = 0.218$ for the maximal height of standing waves and claimed that these highest waves have a peak angle of 90°. This gives the surface particle at the peak zero pressure gradient, so it falls freely under gravity at the instant of maximal height. Taylor[4] investigated the highest standing deep-water wave experimentally. Taylor provided support for the right-angle surface peak, but it remained a somewhat controversial result. The assertion of the 90° peak angle for the highest wave originating from Penney & Price[6] was confirmed theoretically by Grant[7] and later by Okamura[8–10], among others. Figure 1 is the preview result of this paper, comparing our work against Taylor's experiments.

Sharp peaks are often seen in breaking processes of ocean waves. At length scales where surface tension can be neglected, a fluid particle at a sharp peak will be in free fall, since the pressure gradient is zero there. Villermaux and Pomeau[11] were able to generate free-surface accelerations above the threshold of gravity inside a vertical tube of variable cross-section. They speculated whether suction (negative pressure) could take place in violent water waves to induce crest accelerations exceeding free fall, but they doubted that it could be observed. We will consider a sharp crest to be released into initial free fall, being independent of the sign of the pressure inside the crest.

A peak angle of 90° for symmetric standing waves allows a maximal slope angle of 45°, which is a 50 percent greater slope angle than the steepest slope of 30° for progressive waves, found by Stokes[1]. Therefore, maximum wave height measured by wavelength (H/L) should be approximately 50 percent greater for standing periodic waves than for traveling waves. This simple estimate holds remarkably well. For standing deep-water waves the analysis by Schwartz & Whitney[12] gave the constraint $0.204 < H/L < 0.213$, while Tsai & Jeng[13] established $H/L = 0.204$, confirmed by Tsai *et. al.*[14]. The earlier result of $H/L = 0.203$ by Grant[7] still rivals the recent work in explaining the classical experiments[4], as it was obtained analytically from first principles. As anticipated, these results are close to 50 percent greater than the established value of $H/L = 0.1412$ for traveling deep-water waves[3].

The class of nonlinear standing waves that obeys the restriction of strict periodicity in time needs to be based on strict periodicity in space. Such a classification applies only to two-dimensional flow in a rectangular container, which is equivalent to infinite horizontal extent with a given wavelength. When we scrutinize the highest standing wave, full

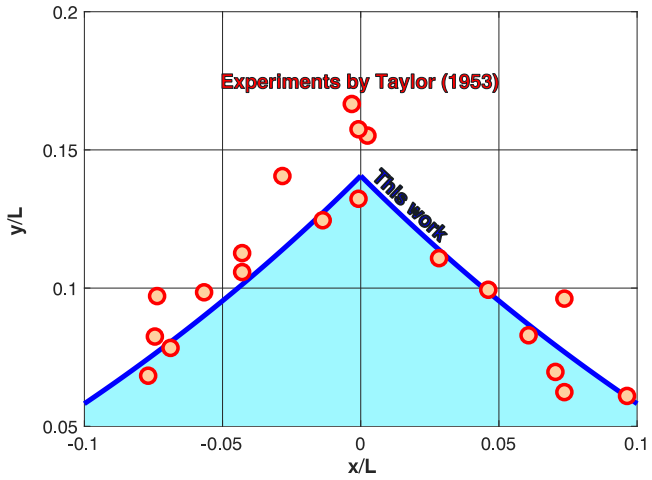

FIG. 1. A preliminary illustration of our analytical solution for the highest wave peak, in comparison with the classical experiments by Taylor[4].

free-surface nonlinearity must be taken into account. A lasting challenge is to make a distinction between standing waves that are strictly periodic in time and those that deviate from strict temporal periodicity. Only waves with a smooth initial shape may evolve into a strictly time-periodic flow after having been released. Standing waves close to the theoretically highest configuration with an instantaneous sharp peak are therefore expected to deviate from strict periodicity in time, which has been confirmed by precise numerical work[15]. These authors demonstrated lack of convergence of high-order series expansions in space and time upon approaching a peaked surface of maximal elevation.

In general, there are three basic approaches to modeling the highest standing wave with a given wavelength, applying the full nonlinear free-surface conditions.

(i) Restricting the modeling to strictly time-periodic flow. This was first done by Penney & Price[6], who tried to achieve a solution that combined a peaked surface shape with their assumption of strict periodicity in time. The sharp peak could not be reached because of the Gibbs phenomena of the truncated Fourier series, so a local analysis was added for the peak. Longuet-Higgins & Dommermuth[16] challenged the assumption of periodicity in time with efficient numerical integration in time and full free-surface nonlinearity. They identified hysteresis loops of non-reversibility for elevation amplitudes close to maximal, revealing inconsistency in the time-periodicity assumed by Penney & Price[6] for high surface elevations.

(ii) To treat the highest standing wave as an initial value problem where a deformed surface is released from rest to flow under gravity. This is a nonlinear Cauchy-Poisson problem of the first category, where there is nonzero initial elevation combined with zero initial velocity. This approach was introduced by Grant[7], and he studied the initial acceleration flow with the exact nonlinear dynamic condition. His work has hardly been followed up, in spite of the fact that his calculated surface shape fits better to the experiments by Taylor[4] than all competing theories. Grant's[7] idea of releasing a deformed surface shape from rest under gravity was followed up by Spielvogel[17], modeling the ultimate stages of the run-up of a solitary wave along a slope.

(iii) To treat the highest standing wave as a state of maximal potential energy having evolved from an initially forced flow. This is a nonlinear Cauchy-Poisson problem of the second category, where there is zero initial elevation combined with a nonzero initial velocity. This approach was first applied by Saffman & Yuen[18], but their computed standing waves showed quite large deviations from exact periodicity in time. A similar work by Longuet-Higgins & Dommermuth[16] gave great improvements in numerical accuracy. These authors were able to compute a fully nonlinear standing wave with 84 percent of the elevation of the idealized highest peaked wave calculated by Grant[7]. They studied the evolution of energetic standing oscillations beyond the amplitude limits of time-periodic waves. Such flows will evolve high and narrow peaks which will fragment and break as they start their downward motion.

Our present work starts with the assumption by Grant[7] of a motionless state of pure acceleration. We add the first-principle basis of assuming only one length scale for the peaked highest standing wave. Moreover, we will arrive at an analytical formula for the surface shapes, where the peaked shape is the highest member of a family of shapes. We will provide a link to[16] by comparing their highest periodic wave with a member of our stagnant waves with the above-mentioned 84 percent amplitude of the peaked highest wave.

The structure of the paper is organized as follows. Section 2 formulates our nonlinear theoretical model. The initial surface shape of the highest standing deep-water wave is investigated in Section 3. Section 4 presents physical length scales at finite depth before general discussions and conclusions in Section 5. Appendix A provides a complex analysis for the surface peak. Appendix B is dedicated to the highest non-breaking rogue wave.

II. FORMULATION OF THE THEORETICAL MODEL

The early papers (Penney & Price[6], Tadjbakhsh & Keller[19]) indicated the existence of nonlinear standing waves with strict periodicity both in space and time, up to some threshold amplitude. Later work confirmed this periodicity for standing waves on deep water, see Vanden-Broeck & Schwartz[20], Schwartz & Whitney[12], and Tsai & Jeng[13]. This strict periodicity up to a certain amplitude threshold was not proven but assumed, yet the good agreement between the different approaches makes its existence credible, as far as infinite depth is concerned.

Strictly time-periodic standing surface waves in an inviscid fluid need to be reversible in time, which they can only be if the highest elevation $y=\eta(x,0)$ is motionless. Any nonzero surface velocity $\partial\eta/\partial t(x,0)$ would imply that the opposite surface flow $-\partial\eta/\partial t(x,0)$ was also legitimate. Such a time-periodic standing wave with peaked amplitude would not be unique, and a family of Fourier potentials with different phase shifts between surface velocity and surface elevation would be constituted. Existing work gives no indication that a family of time-periodic surface shapes with different phase shifts exists. Without such phase shifts, the different periodic deep-water standing waves will be a one-parameter family of reversible flows, to be represented only by the flow amplitude when the wavelength is given. Thus we consider a situation where a free-surface flow has come to rest with a deformed free surface. We look at the situation just before or just after the instant $t=0$, where the velocity field is assumed to be zero everywhere. The inviscid and incompressible fluid (liquid) is initially at rest with a deformed free surface given by $y=\eta(x,0)$. The constant fluid density is ρ, and g is the uniform gravitational acceleration.

The 2D fluid domain is the vertical x,y plane. The free surface has constant atmospheric pressure. Time is denoted by t. The y axis is directed upwards in the gravity field, and the horizontal x axis is parallel to the undisturbed free surface. The velocity vector is $\vec{v}$. The position of the free surface is $y=\eta(x,t)$. The elevation $\eta(x,t)$ is measured with respect to an undisturbed surface level $y=0$. At the instant $t=0$, the fluid is at rest, implying

$$\vec{v}=\nabla\times\vec{v}=0,\ \ t=0. \tag{1}$$

No vorticity is generated within the inviscid fluid, and the flow remains irrotational according to Lord Kelvin's theorem

$$\nabla\times\vec{v}=0, \tag{2}$$

for all times when there is free-surface flow, so we take the time derivative to get

$$\nabla\times\frac{\partial\vec{v}}{\partial t}=0. \tag{3}$$

This is the local acceleration at all times, but at $t=0^+$ it is the total acceleration. The released flow at $t=0^+$ has an irrotational acceleration field, with an initial acceleration potential $\phi(x,y)$ where $\partial\vec{v}/\partial t|_{t=0^+}=\nabla\phi$. The incompressible flow satisfies Laplace's equation

$$\nabla^2\phi=0, \tag{4}$$

in the entire fluid domain. The free surface is assumed to be initially at rest

$$\left.\frac{\partial\eta}{\partial t}\right|_{t=0}=0, \tag{5}$$

which is equivalent to the above assumption that the entire fluid is at rest at $t=0$

$$\vec{v}|_{t=0}=0. \tag{6}$$

From the conservation of momentum, Bernoulli's equation follows

$$\frac{p-p_{atm}}{\rho}+\phi+gy=0, \tag{7}$$

valid at $t=0$ when the convective acceleration is identically zero. The pressure is p, and the atmospheric pressure is p_{atm}. With zero initial velocity, the initial (nonlinear) dynamic free-surface condition is

$$\phi+gy=0,\ \ y=\eta(x,0), \tag{8}$$

neglecting surface tension. Our idealized model represents an instantaneous state of rest where the entire energy is gravitational potential energy. From a state of rest with a deformed free surface, the early linearized flow for $t>0$ is the same (with a sign reversal for the velocity) as the late flow for small negative values of t.

We may redefine this reference level by an adjustment height Δy so that the appropriate transformation $y\to y-\Delta y$ allows $y=0$ to represent the undisturbed free surface. This is done by the definition

$$\Delta y=\frac{1}{\lambda}\int_0^\lambda\eta(x,0)dx. \tag{9}$$

The potential energy E contained in the deformed free surface is given by

$$E=\rho g\int_S\frac{\eta(x,0)-\Delta y}{2}dS \tag{10}$$

measured per length unit perpendicular to the vertical x,y plane. Here $(\eta(x,0)-\Delta y)/2$ is the mass centre of an area element $dS=(\eta(x,0)-\Delta y)dx$ of fluid above the reference level

$y = \Delta y$. The area S is limited by one wavelength $-\lambda/2 < x < \lambda/2$.

Linearized theory gives an automatic mass balance at the undisturbed level $y = 0$, whereby $\Delta y = 0$, abolishing surface adjustment. The formula for the potential energy E within a wavelength is

$$E_{lin} = \frac{1}{2}\rho g \int_{-\lambda/2}^{\lambda/2} \eta(x,0)^2 dx, \tag{11}$$

according to linearized theory. From now on, we work with dimensionless variables. These are gravitational units, obtained by putting $g = 1$ and $\rho = 1$ in the energy formulas. The wavelength λ of the nonlinear standing wave is scaled as 2π dimensionless units, whereby the dimensionless wavelength is $L = 2\pi$, corresponding to a unit dimensionless wave number in the x direction. Thus we have the general transformations

$$\left(\frac{x}{\lambda}, \frac{y}{\lambda}\right) \to 2\pi(x,y), \tag{12}$$

from the coordinates with dimension to the dimensionless coordinates. The horizontal unit wavelength that we study will thus appear as $-\lambda/2 < x < \lambda/2$ in coordinates with dimension and $-\pi < x < \pi$ in dimensionless coordinates.

We will model the highest wave with a sharp surface peak. The peak itself has no length scale since its radius of curvature is zero. Thereby, it is possible to have only one length scale for the highest standing deep-water wave.

III. THE INITIAL SURFACE SHAPE

Since Lord Rayleigh's early work[5], many approaches have aimed at describing the highest standing wave, in combination with its time dependence. We will consider the highest wave as an initial surface shape released from rest under gravity, taking advantage of reversibility through the instant $t = 0$. We will start with some elementary geometric considerations based on dimensional analysis. Our basic postulate is that the highest standing deep-water wave has only one length scale.

A. The primitive model with one single length scale

The idealized peaked surface shape has a single precise length scale. When we disregard the constraints on the instantaneous acceleration flow field, the radius of curvature for the surface contour presents itself as the single length scale. Thus the primitive model for the surface is the circular arc with constant dimensionless radius R, illustrated in Figure 2. We consider two neighboring circle arcs with centers in the points

$$(x,y) = \left(\pm\frac{R}{\sqrt{2}}, \frac{R}{\sqrt{2}} + \eta_{max}\right), \tag{13}$$

Two circle arcs from these centers will compose two wavelengths of this idealized periodic peaked surface. Each peak has a right angle, which we will substantiate in the Appendix. The three neighbouring highest peaks are located in the points $(-L, \eta_{max})$, $(0, \eta_{max})$ and (L, η_{max}). The fixed peak angle of $\pi/2$ sets the geometric constraint

$$R = \frac{L}{\sqrt{2}} = \pi\sqrt{2}. \tag{14}$$

The ratio $\sqrt{2}$ between the wavelength and the radius of curvature is consistent with our postulate of one joint length scale for the surface contour.

The constraint of zero average water level implies the relationship

$$\eta_{max} L = \left(\frac{\pi}{4} - \frac{1}{2}\right) R^2. \tag{15}$$

implying that

$$\eta_{max} = \left(\frac{\pi}{8} - \frac{1}{4}\right) L = \left(\frac{\pi}{4} - \frac{1}{2}\right) \pi, \tag{16}$$

with dimensionless units. The elementary estimate for the total wave height of the peak is $H = R(1 - 2^{-1/2})$. Thereby, we have the simplest possible estimate for the relative wave height

$$\frac{H}{L} = \frac{\sqrt{2}-1}{2} = 0.2071. \tag{17}$$

Remarkably, this simple estimate differs less than two percent from the established results mentioned in the introduction. This reasonable agreement serves as a qualitative confirmation of our above postulate of a single length scale for the stagnant surface peak. Figure 3 compares our primitive circle estimate for the surface elevation with the exact peaked surface shape calculated by Grant[7]. Subfigure 3 (a) shows how the primitive circle estimate of the surface elevation deviates from the exact surface contour. Subfigure 3 (b) shows the radius of curvature $R(x)/L$, which has to vary continuously in order to satisfy Laplace's equation according to exact nonlinear theory, while it has the constant value 0.7071 in the primitive circle estimate. The two subfigures reveal that the primitive circle model overestimates the peak height as well as the curvature around the peak. We also note that the average surface level and the average radius of curvature in the exact model are fairly close to the respective values from the primitive circle estimate for the surface contour. Here Laplace's equation appears to be an agent of averaging, in agreement with Green's identities of potential theory. This apparent averaging may be interpreted as taking care of our single length scale postulate. In Figure 3, we anticipate our own analytical formula for the surface shape, and also Figure 8 below, where we will compare the circle estimate with other approximations from the literature.

We realize that a strict single-length-scale postulate can be posed only for the horizontal direction since the initial flow field must be allowed to satisfy Laplace's equation for the acceleration potential. The right-angle peak of the primitive

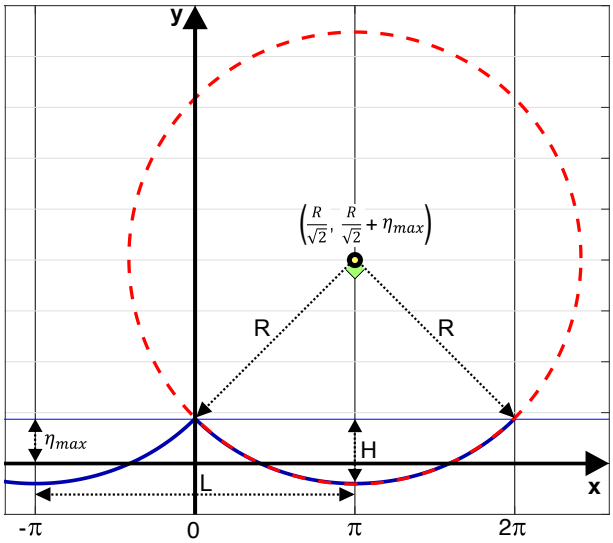

FIG. 2. An illustration for our elementary estimate (primitive model) where the highest stagnant wave surface is represented as a quarter circle arc. This is the simplest possible version of postulating one single length scale for the highest wave. The relevant parameters are included in this figure. The wavelength is $L = 2\pi$. The constant radius of curvature is $R = \sqrt{2}\pi$. The total wave height is H. The peak elevation is η_{max}.

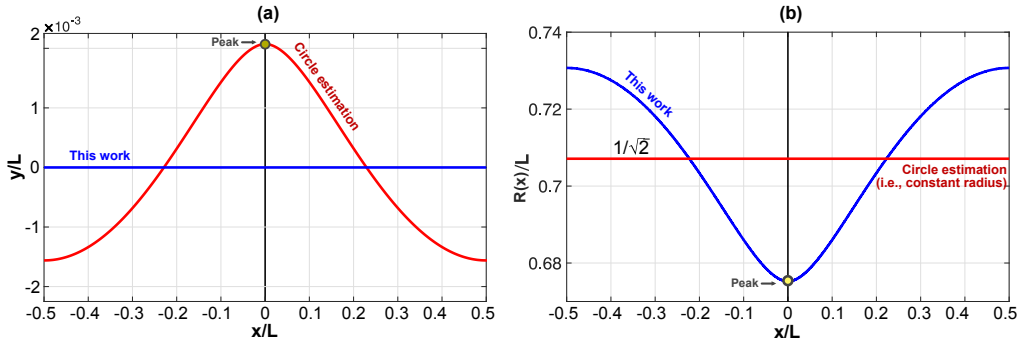

FIG. 3. Two comparisons between the elementary circle estimate (primitive model) for the peaked surface and our single Fourier component solution below coincide with Grant[7]. **(a)** A subfigure for the surface elevation $\eta(x,0)$. The blue curve shows the deviation (in the vertical direction) of the circle from the Fourier component solution. The wavelength L represents the length unit in this plot. **(b)** A subfigure for the radius of curvature $R(x)/L$. It varies continuously according to the exact theory. In the elementary circle estimate, it has the constant value $R/L = 1/\sqrt{2} = 0.7071$.

model sets the exact circle radius $R = L/\sqrt{2}$ once the wavelength L is given, leaving no flexibility for solving a boundary value problem to determine the free surface shape. Moreover, we include one single Fourier term horizontally to solve Laplace's equation exactly and avoid compromising our postulate of a single length scale.

The primitive estimate in Eq. (17) for the relative wave height can be put in perspective by carrying out the same arguments for the peaked Stokes wave with slope angle $\pi/6$. Thereby the circle arc radius is equal to the wavelength ($R = L$), which immediately gives $H/L = 1 - \sqrt{3}/2 = 0.13397$. This crude approach leads to a value for the relative wave height, which differs by only five percent from the established value $H/L = 0.1412$[3]. Replacing the highest Stokes wave pro-

file with a circular arc is an oversimplification. Nevertheless, it gives a simple analytical result for the wave height ratio between standing Stokes waves (present problem) and propagating Stokes waves

$$\frac{H_{standing}}{H_{propagating}} = \frac{\sqrt{2}-1}{2-\sqrt{3}} = 1.5459, \tag{18}$$

comparable with other estimates from the literature. The Fourier series solutions by Penney & Price[6] gave the first prediction of 1.53 for this ratio. The work by Grant[7] leads to the ratio

$$\frac{H_{standing}}{H_{propagating}} = \frac{0.20347}{0.1412} = 1.4410, \tag{19}$$

when it is combined with the established result[3] for propagating waves: $H_{propagating}/L = 0.1412$. The primitive circle estimate in Eq. (18) over-predicts this ratio by merely seven percent.

B. Analytical solution for the surface profile

The dimensionless version of the dynamic condition in Eq. (8) is

$$\phi + y = 0, \;\; y = \eta(x,0), \tag{20}$$

valid at the initial instant $t = 0$. In Appendix A, we formulate a complex version of this condition. By a simple, complex analysis for the peaked surface, we show that the instantaneous surface of a periodic standing wave has a right angle at its highest peak. Thereby we support Penney & Price[6] in their claim of a right-angle surface peak, recalling the reservation that their assumed time-periodicity is not proven.

Like Grant,[7] we search for the highest standing wave with a surface peak. In the main text, we consider the instantaneous acceleration potential at $t = 0$, which will have the general form

$$\phi(x,y,0) = \sum_{n=1}^{\infty} A_n(0)\cos(nx)e^{ny}. \tag{21}$$

The leading term (with $n = 1$) in this Fourier series has wavenumber 1 in the horizontal direction, setting the dimensionless wavelength $L = 2\pi$ as a length scale. The flow field in the vertical direction is a potential flow adjusted to the sinusoidal variation in the horizontal direction. The only way of maintaining our strict postulate of one length scale only is to take a single horizontal Fourier mode as the exact solution

$$\phi(x,y,0) = A\cos(x)e^{y}. \tag{22}$$

We neglect all terms $n \geq 2$ in the Fourier series of Eq. (21) to suppress all shorter length scales. Our single length scale postulate for the peaked surface does not make any assumption concerning the peak angle. Its zero radius of curvature prevents the peak from having a local length scale of its own.

Our postulated exact solution in Eq. (22) loses its link to the level $y = 0$ as an undisturbed water level, which is a relict from linear theory. This is because the dynamic condition of Eq. (20) is essentially nonlinear. Therefore, we are free to adjust the water level by an amount Δy for setting the average water level, knowing that $\Delta y = 0$ applies only to linearized theory. This is a subtle departure from the approach by Grant[7], where he tried to save $y = 0$ as a reference level also for his finite-amplitude solution. Then he had to perform a pragmatic adjustment of his zero elevation level, which he did by calibrating the peak point to experimental data from Taylor[4].

Our single-length scale postulate is supported by the fact that no physical causes are known for generating competing length scales. Mathematical models or methods that do not allow a sharp surface peak cannot avoid producing other length scales in addition to the wavelength, which is exemplified by Wilkening[21]. Nevertheless, it is not a physical argument against our single length scale that a chosen mathematical description does not allow it. A narrow surface peak that is mathematically rounded instead of sharp surrounds itself with surface undulations that tend to be mathematical artifacts since they lack satisfactory causal explanations.

The only acceleration potential consistent with our postulate is, therefore, the single Fourier mode. The complex version of Eq. (22) is

$$\Phi(z,0) = Ae^{-iz}, \tag{23}$$

analytically extending the real acceleration potential ϕ into the complex z plane where $z = x + iy$. The imaginary unit is i.

We insert the potential of Eq. (22) into the dynamic free-surface condition of Eq. (20), where we let the amplitude A obey the condition $0 < |A| \leq |A_{max}|$. Thereby, we define a one-parameter family of finite-amplitude stagnant free-surface shapes with A as their parameter. For each legal value of A, applying $\phi + y = 0$ using Eq. (22), we then have the stagnant surface contour $y = \eta(x,0)$, given by the inverse functional relationship

$$x = \arccos\left(-\frac{y}{Ae^{y}}\right). \tag{24}$$

We have not adjusted the surface level, $y = 0$, and it does not represent the undisturbed water level in Eq. (24). Furthermore, we provide the peaked free-surface shape, $y = \eta(x,0)$, by the implicit analytical solution of the non-adjusted y for Eq. (24) as follows

$$y = -W\Big(A\cos(x)\Big). \tag{25}$$

In this formulation, the Lambert W function, $W(z) = w$, is defined by the equation

$$we^{w} = z. \tag{26}$$

Thus we express a standing Stokes wave by the Lambert W-function, while Jordan[22] applied this function to a traveling Stokes wave. The dimensionless adjustment height can now be found from Eq. (9) using Eq. (25) as follows

$$\Delta y = \frac{1}{2\pi}\int_{-\pi}^{\pi} \eta(x,0)dx = -\frac{1}{2\pi}\int_{-\pi}^{\pi} W\Big(A\cos(x)\Big)dx, \tag{27}$$

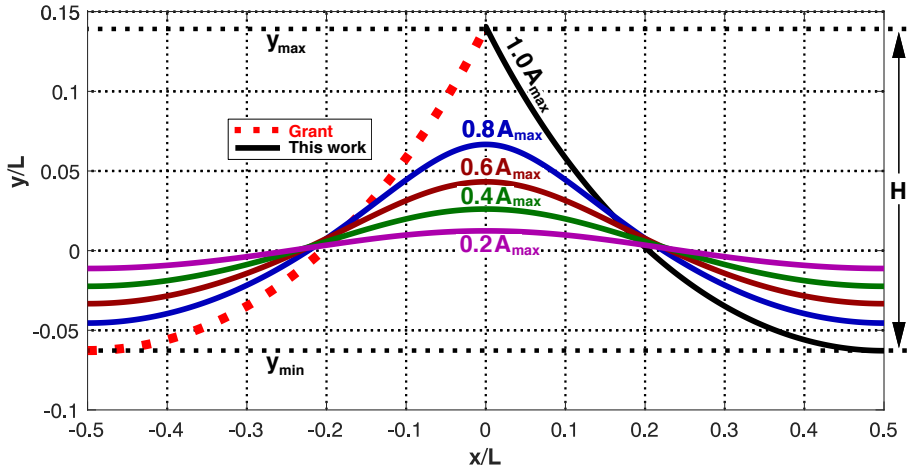

FIG. 4. Family of stagnant surface profiles with different amplitudes. The acceleration amplitudes are given as fractions of the maximal amplitude $|A_{max}| = 1/e$. Negative values of the acceleration potential amplitude A are chosen for locating each surface crest at $x = 0$. Each surface level is here adjusted by an amount Δy so that $y = 0$ is the undisturbed free surface. A similar plot by Grant[7] is included on the left-hand side for the peaked surface, but it had to be shifted vertically to match our work. Both axes scaled by the wavelength $L = 2\pi$.

TABLE I. Dimensionless parameters for the stagnant wave for different acceleration potential amplitudes A, given as fractions of the maximal amplitude A_{max}, where $|A_{max}| = 1/e$ is the amplitude of the peaked highest wave. The lengths are measured by is the dimensionless wavelength 2π. The highest and lowest surface levels, the adjustment height Δy and the maximal wave height $H = y_{max} - y_{min}$ are calculated. The predicted wave height H_{lin} according to linear theory is $H_{lin}/L = A/(A_{max}\pi e)$. The dimensionless potential energy E is calculated and compared with its value E_{lin} according to linear theory. The maximal slope angle $|\theta_{max}|$ and its horizontal coordinate are tabulated.

A	y_{max}/L	y_{min}/L	$\Delta y/L$	H/L	H_{lin}/L	E	E_{lin}	$\lvert x\rvert_{\theta,max}$	$\lvert\theta_{max}\rvert$
$1.0A_{max}$	0.14063	-0.06284	0.01852	0.20347	0.11710	0.42906	0.21258	0.0000	45.0000°
$0.967A_{max}$	0.10584	-0.05873	0.01556	0.16457	0.11324	0.34689	0.19879	0.0735	31.7743°
$0.8A_{max}$	0.06669	-0.04548	0.00837	0.11217	0.09368	0.18154	0.13605	0.1350	20.6985°
$0.6A_{max}$	0.04320	-0.03331	0.00408	0.07652	0.07026	0.08801	0.07653	0.1727	13.9178°
$0.4A_{max}$	0.02610	-0.02238	0.00180	0.04849	0.04684	0.03601	0.03401	0.2013	8.7628°
$0.2A_{max}$	0.01240	-0.01121	0.00027	0.02361	0.02342	0.00862	0.00850	0.2264	4.2544°

but it must be evaluated numerically for each given amplitude. Therefore, we choose to keep the non-adjusted level $y = 0$ in all our analytical formulas. Without adjustment, the horizontal coordinates that give $\eta(x,0) = 0$ are $x/L = \pm 0.25$, which follows from Eq. (24) and is identical to the value from linear theory. Our numerical value for the adjustment height of the peaked highest wave is $\Delta y/L = 0.01852$, and it displaces the points of zero elevation to their supposedly correct locations $x/L = \pm 0.2047$. In Figure 4, we take the curve from Grant[7] and corrects it by adjusting it by our value $\Delta y = 0.01852L$, not by his own pragmatic fit to the highest experimental point by Taylor[4]. Grant[7] did not report his chosen value for Δy, but from his plot we estimate the value $x/L = 0.24$ where the surface elevation is supposedly zero. It is not even close to providing a mass balance between the deformed free surface and its undisturbed reference level.

The peaked surface obeys the dynamic condition of Eq. (20), with an additional constraint

$$\frac{d}{dz}(\Phi - iz) = 0, \tag{28}$$

at the peak point (see Appendix A). Thereby, we determine the maximal amplitude $|A|_{max}$. We choose $A < 0$, so there is a central peak point $z = i\eta(0,0)$, where we have

$$\frac{d\Phi}{dz} - i = -i\Phi - i = 0, \;\; z = i\eta(0,0) = i\eta_{max}, \tag{29}$$

according to Eq. (28). At the peak point, $(x,y) = (0,\eta_{max})$, we thus have $\Phi = -1$, constraining the initial acceleration amplitude

$$A = -e^{-\eta_{max}}. \tag{30}$$

The minus sign means that the peak falls freely under gravity. The surface peak obeys the dynamic condition, Eq. (20),

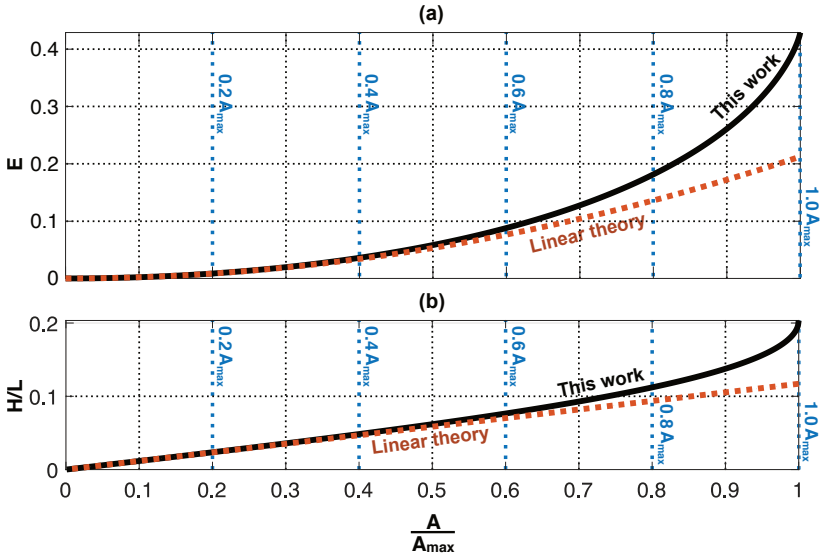

FIG. 5. Comparison of this work assessed against linear theory (red dotted line) as function of amplitude A. **a)**: Dimensionless potential energy E calculated by eq. (41). **b)**: Dimensionless wave height relative to wavelength (H/L) calculated by eq. (36).

where we insert A to get

$$y_{max} = \eta(0,0) = 1. \tag{31}$$

Plugged back into Eq. (30), this gives $1 = -W(A)$ with the acceleration amplitude given as follows

$$|A_{max}| = \frac{1}{e} = 0.367879. \tag{32}$$

Choosing the negative value $A_{max} = -1/e$ will give a single central surface peak at $x = 0$. If we instead choose the positive value $A = 1/e$, we get two half peaks completing a wavelength at $x = \pm\pi$. We will present figures with each of these sign options.

Choosing a central peak with $A = -1/e$, the troughs with the minimum value $y_{min} = \eta(0,\pi)$ obey the relationship

$$|y_{min}| + \log|y_{min}| = -1, \tag{33}$$

in agreement with Eq. (25). This trough elevation y_{min} is evaluated as

$$y_{min} = \eta(\pi,0) = -W(-A) = -0.278465. \tag{34}$$

The adjusted levels of crest and trough for the highest wave are then

$$y_{min} = -W(-A) - \Delta y, \quad y_{max} = -W(A) - \Delta y, \tag{35}$$

where Δy is found from Eq. (9). This adjustment is needed to redefine $y = 0$ as the undisturbed free surface. The height difference is independent of Δy, yielding

$$H = y_{max} - y_{min} = W(-A) - W(A). \tag{36}$$

The insertion for the maximum amplitude into Eq. (36), normalized by $L = 2\pi$, yields

$$\frac{H_{max}}{L} = \frac{W(-A_{max}) - W(A_{max})}{2\pi} = \frac{W\left(\frac{1}{e}\right) - W\left(-\frac{1}{e}\right)}{2\pi} \approx 0.20347. \tag{37}$$

The steepness $|dy/dx|$ of the free surface is found from Eq. (24)

$$\left|\frac{dy}{dx}\right| = \frac{\sqrt{A^2e^{2y} - y^2}}{y-1}, \tag{38}$$

where y is non-adjusted. The surface slope angle is $\theta = \arctan(|dy/dx|)$. To find the inflection point with maximum steepness, it follows from implicit differentiation that

$$\frac{d^2y}{dx^2} = \frac{A^2e^{2y}(y-2) + y}{(y-1)^3} = 0. \tag{39}$$

The non-adjusted value of y as functions of A, at maximum steepness, can be found from

$$A^2 = \frac{y}{(2-y)\,e^{2y}}. \tag{40}$$

Table 1 represents five stagnant surface contours corresponding to equal increments in the amplitude $|A|$. This family of surface contours is also plotted in Figure 4. These surface shapes are not snapshots of oscillating waves but a set of stagnant surface shapes for a simple Fourier potential obeying the exact nonlinear dynamic condition at the free surface.

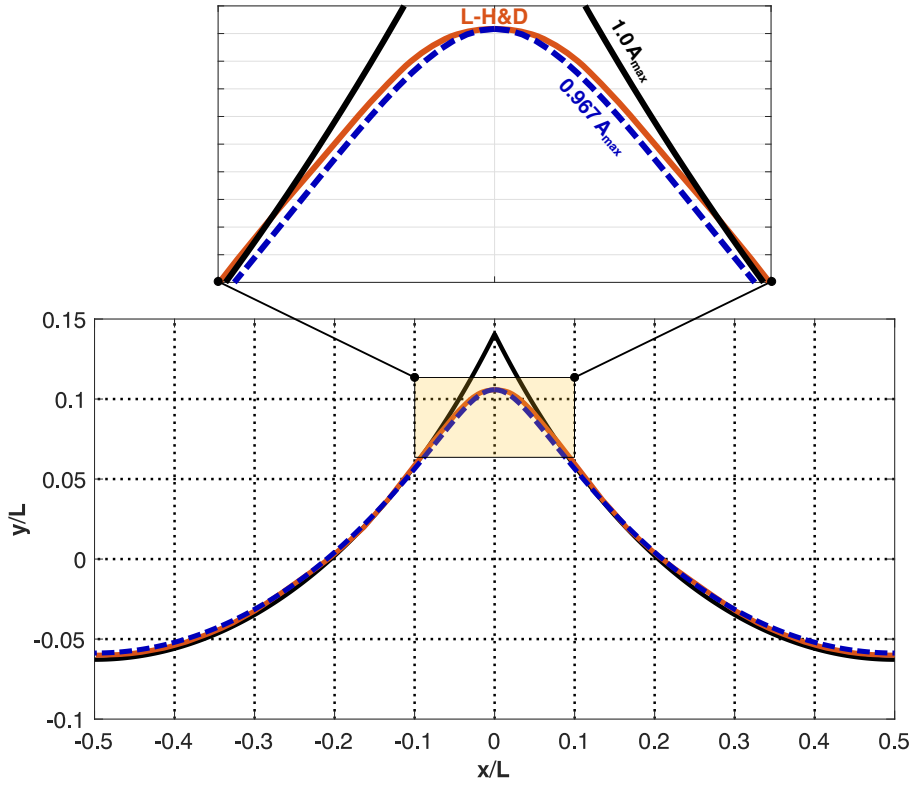

FIG. 6. The highest wave profile among those computed by Longuet-Higgins & Dommermuth[16] that gave an evolution close to periodic time dependence is here reproduced (from their Figure 1, here marked with L-H&D). We include our peaked highest wave, coinciding with the profile found by Grant[7], after adjusting its average water level zero. For direct comparison with these reproduced numerical results[16], a member of our family of smooth wave profiles is added, hand-picked with a flow amplitude $A = 0.967A_{max}$. Here A_{max} is the reference amplitude for the acceleration potential of the peaked highest wave. The numerical value 0.967 is determined by requiring that our smooth wave profile has a maximum elevation coinciding with the profile found by Longuet-Higgins & Dommermuth[16].

Each isobar that belongs to the peaked highest wave can be reinterpreted as a free surface, since the flow is not changed by adding a uniform pressure everywhere. The family of stagnant surface shapes in Figure 4 corresponds to the set of isobars, with vertical displacements being added so that the average surface level is zero in each case. We find no indication that a suction (negative pressure) can be present for the potential-flow acceleration fields with a free surface, so we rule out the possibility of super free fall from rest[11].

The left-hand side of Figure 4 includes the graph obtained analytically by Grant[7]. It can be shown that our exact solution of Eq. (25) is identical to the solution by Grant[7]. However, he did not consider his solution as exact, only as a one-term Fourier series truncation horizontally. Moreover, he did not compute the adjustment height, which is what we do by Eq. (27). Grant[7] was aware that his plotted solution did not fix the undisturbed water level, but he made the choice of calibrating his theoretical peak point to the peak height found experimentally by Taylor[4]. We see no advantage in a compromised mass balance for benchmarking with a single experimental point, so we will compare Taylor's experimental surface shape with the adjusted theoretical curve with zero average elevation.

Note that our underlying postulate of a single horizontal length scale applies only to the peaked highest wave. The other surface shapes in Figure 4 are merely members of the same one-component Fourier family of shapes, constituted by the peaked highest wave. Each stagnant wave with smaller amplitude possesses several length scales due to the finite curvature at their smooth peaks. The sharp right-angle peak that we calculate has no length scale of its own. Our arguments in favor of a single length scale contrast the sophisticated numerical simulations by Wilkening[21]. He approached the limit-

ing behavior of large-amplitude deep-water standing waves by identifying small-scale phenomena coupling instabilities with nonlinear free-surface effects.

Table 1 shows the levels, y_{max} and y_{min}, for the peak and trough of these stagnant surfaces. The induced wave height, $H = y_{max} - y_{min}$, calculated from Eq. (36), is tabulated, together with its prediction (H_{lin}) according to linear theory. Figure 5 compares the exact wave height with linear theory, which is the reference case with the oscillation frequency given by the standard deep-water dispersion relation. The peaked wave is almost twice as high as its predicted value according to linearized theory. The peak and trough elevations y_{max} and y_{min} are calculated in Table 1 from Eq. (35), including the adjustment Δy. Eqs. (38) and (40) are used to calculate the magnitude ($|\theta_{max}|$) and the position ($x_{|\theta,max|}$) of the maximum steepness angle. Figure 5 also compares the exact potential energy E with its approximation E_{lin} according to linearized theory,

In addition, Table 1 provides the dimensionless potential energy E, measured relative to the adjusted zero level of the undisturbed free surface. E is defined by the dimensionless version of Eq. (41)

$$E = \frac{1}{2}\int_{-\pi}^{\pi} \Big(\eta(x,0) - \Delta y\Big)^2 dx, \tag{41}$$

and it represents the dimensionless potential energy contained in one wavelength λ. A column with the energy E_{lin} according to linearized theory is added to Table 1, showing good agreement with the exact theory for the lowest flow amplitude $A/A_{max} = 0.2$. The unit of energy is $8\pi^3\rho g\lambda^3$, given per length unit perpendicular to the x,y plane.

Table 1 includes results for the special case $A = 0.967A_{max}$, which refers to the smooth wave shape included in Figure 6 for close comparison with the highest time-periodic wave computed by Longuet-Higgins and Dommermuth[16]. Their computed maximal slope angle of 32° is in excellent agreement with our value 31.77°. Our result is exact as far as it is analytically based, but it rests on the numerically estimated flow amplitude $A = 0.967A_{max}$ to fit with the highest elevation for almost-periodic waves included in[16].

The linearized version of the surface elevation is simply

$$\eta(x,0) = |A|\cos(x). \tag{42}$$

The dimensionless version of the linearized energy formula of Eq. (11) is

$$E_{lin} = \frac{1}{2}\int_{-\pi}^{\pi} \eta(x,0)^2 dx = \frac{\pi}{2}A^2 = \frac{\pi}{2e^2}\left(\frac{A}{A_{max}}\right)^2. \tag{43}$$

Our peaked surface profile of the highest wave amplitude is assessed graphically against the experiments of Taylor[4] and competing analytical models. Figure 7 depicts the surface profiles, whereas Figure 8 assesses the local height difference of the other work measured relative to the present model. It is worth noting that one set of the experiments of Taylor[4] agrees better than the second set. The second set seems to have a greater deviation in precision.

C. Deep-water waves with quasi-periodicity in space

Traditional approaches to standing deep-water waves assumed periodicity in space and time. While periodicity in space could be taken as a constraint for the mathematical model, periodicity in time remained an uncertain assumption for large standing waves. Since the pioneering work[6], clarifications concerning the validity of periodicity in time had been in demand. A final breakthrough came with the work by Longuet-Higgins and Dommermuth[16], who settled that standing waves with amplitudes near the legal maximum do not give time-periodic motion. This is of course also true for the peaked stagnant wave. It nevertheless remains a physically valid initial condition, which we investigate along the lines of Grant[7]. The precise work by Williams *et al*.[15] confirmed that standing waves close to a peaked shape cannot be periodic in time. The early behavior of these extreme standing waves after being released from rest was not addressed by these authors[15].

Taylor[4] limited his laboratory work to a single wavelength. However, an experimental standing wave that covers several wavelengths cannot be exactly periodic is space. It is therefore of interest to perform a deviation from the strict requirement of spatial periodicity, referring to the recent work by Wilkening and Zhao[24] on traveling Stokes waves with quasi-periodicity.

As an extension of our model for standing Stokes waves, we will for a moment replace the single Fourier mode in eq. (22) with a combination of two Fourier modes for the acceleration potential

$$\phi(x,y,0) = A\cos(x)e^y(1 + \varepsilon\cos(x/4)e^{y/4}), \tag{44}$$

where ε is of order smaller than one. We thus consider a spatial carrier wave with a small modulation. We handpick the modulation wavelength to be four times that of the carrier wave. Thereby we let the single length scale postulate retain approximate validity locally, which means that we disregard all higher harmonics of the carrier wave.

In Figure 9 we plot one example of this quasi-periodic stagnant standing wave. We choose $\varepsilon = 0.2$, and compute the maximal amplitude $|A|_{max} = 0.293$ that gives a peaked surface at $x = 0$. We plot the initial free surface and some of the subsurface isobars for a full wavelength $-4\pi < x < 4\pi$. There are lower (smooth) surface crests surrounding the central sharp peak. The surface crests and troughs are approximately (not exactly) located at $x = n\pi$, where n is an integer. Due to the chosen symmetry, the central peak is located at $x = 0$, and the lowest crests are located at $x = \pm 4\pi$.

The position of the central peak is $(0, \eta(0,0))) = (0, 0.95163)$. It is surrounded by two neighboring troughs at $(\pm 3.1125, -0.25686)$. Their positions deviate somewhat from $x = \pm\pi$ due to the quasi-periodicity within a full wavelength 8π. In Figure 9 we do not adjust the surface level to provide mass balance. It is not needed for extracting a key result: The wave height to wavelength ratio for the modulated wave around its peak at $x = 0$

$$\frac{\eta(0,0) - \eta(\pm 3.1125, 0)}{2 \times 3.1125} = \frac{1.20849}{6.225} = 0.194. \tag{45}$$

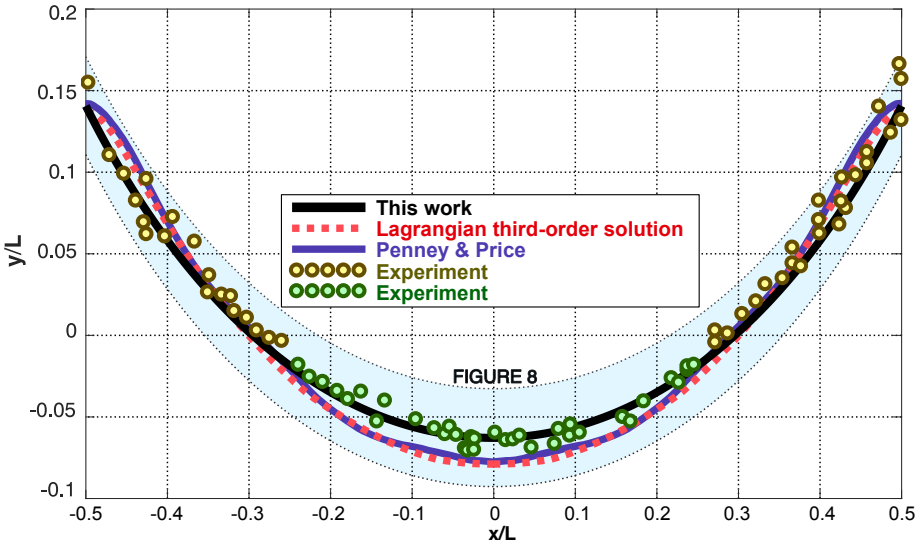

FIG. 7. Three sets of theoretical predictions for the highest standing wave, plotted together with experimental points from Taylor[4]. Taylor reported two sets of experiments, marked with different colors. The theoretical graphs follow the set-up from Chen *et. al.* (2009)[23]. Their third-order Lagrangian solution is given by the dotted line. The 5th order Eulerian solution from Penney & Price[6] is given by the solid blue curve, while our present theory is shown by the black solid curve. The light blue envelope will be exported to Figure 8. Axes scaled by $L = 2\pi$.

We note the small deviation that this chosen quasi-periodicity gives from the value 0.20347 of strict periodicity[7]. It contrasts the fact the the peak height 0.95163 is much greater than the other crests with heights 0.46963 and 0.31456. It illustrates a robustness of the greatest relative wave height with respect to moderate deviations from spatial periodicity.

IV. ON PHYSICAL LENGTH SCALES AT FINITE DEPTH

Our basic postulate is that the highest standing periodic wave on deep water has only one physical length scale. In Appendix B, we pursue these physical arguments to argue that a single deep-water stagnant wave peak does not have a physical length scale. It sets its own length scale, leading to a similarity solution for a finite-amplitude stagnant rogue wave peak at deep water.

Let us briefly consider the finite-depth version of stagnant periodic water wave, based on the postulate that it has two length scales. The wavelength is one length scale, while the water depth sets a second length scale. As before, we require that the exact acceleration potential is the single Fourier component

$$\phi(x,y,0) = A_1 \cos(kx)\cosh(k(y+1)), \tag{46}$$

in a finite-depth version satisfying the kinematic bottom condition at $y=-1$. This acceleration potential in Eq. (46) is inserted into the nonlinear dynamic condition in Eq. (20) to get

$$A_1(k)\cos(kx)\cosh(k(y+1)) + y = 0, \;\; y = \eta(x,k), \tag{47}$$

prescribing a peaked shape $\eta(x,k)$ for the stagnant free surface, with the appropriate maximal amplitude $|A_1(k)|$. The hyperbolic cosine term introduces the wavenumber k as a secondary vertical length scale, while there is already a unit vertical length scale by the dimensionless gravitational term y. Further elaboration of the two length scales is achieved by redefining the dimensionless variables

$$(kx, ky, k\eta) = (\tilde{x}, \tilde{y}, \tilde{\eta}), \tag{48}$$

with the dynamic condition in Eq. (47) reformulated as

$$A_1(k)\cos\tilde{x}\cosh(\tilde{\eta}+k) + \frac{\tilde{\eta}}{k} = 0. \tag{49}$$

Now we have a family of peaked surface shapes $\tilde{\eta}(\tilde{x},k)$ dependent on the parameter k, with the appropriate amplitude $A_1(k)$. We introduced a unit wave number in the redefined coordinate system, similar to the deep-water problem in the main text above. The fixed length scale of the wavelength is therefore in place, while the other length scale due to gravity now appears as the parameter k and constitutes a one-parameter family of surface shapes.

In Figure 10 we display the surface shape for infinite depth (here represented as $k \to \infty$), together with one finite value

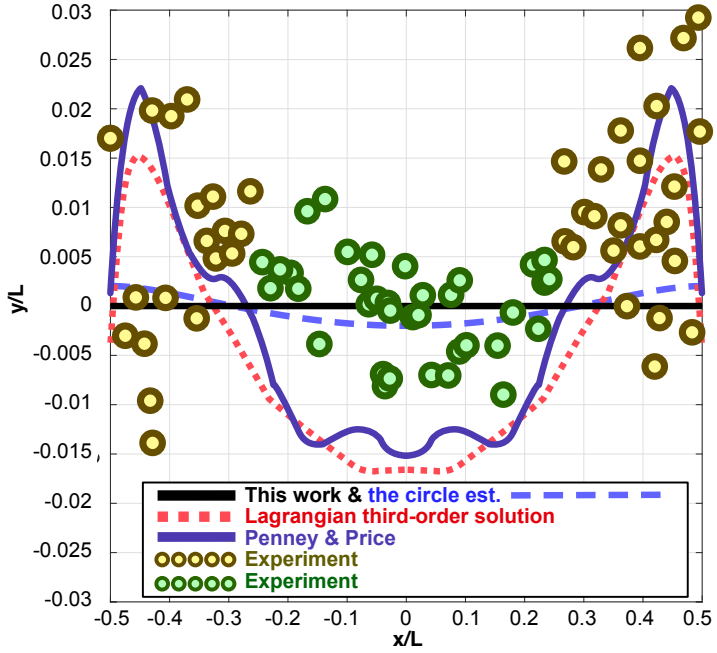

FIG. 8. Error assessment of previous work, imported from Figure 7 (light blue envelope). Now we take our predicted peaked surface elevation $\eta(x,0)$ as the norm, represented by the black line of horizontal zero level. We show the local deviations of earlier work in comparison with our surface contour, measured vertically in length units of the wavelength. The two sets of experimental points from Taylor[4] are marked with different colors. The 3rd order Lagrangian solution from Chen *et. al.*[23] is represented by the dotted line. The 5th order Eulerian solution from Penney & Price[6] is represented by the solid blue curve. We also add our present elementary circle estimate, represented by the dashed blue curve. Both axes are scaled by $L = 2\pi$.

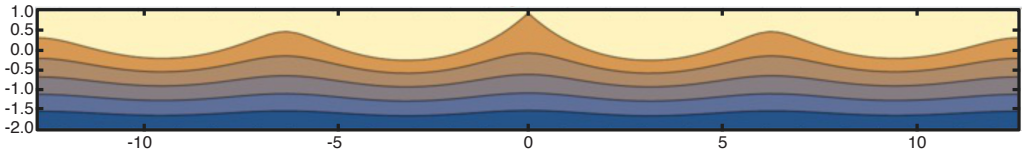

FIG. 9. Stagnant quasi-periodic free surface with a central peak, based on eq. (44). We choose $\varepsilon = 0.2$ and determine numerically the amplitude $A = -0.29307613$ which gives a peaked free surface, where the pressure is zero. Four initial subsurface isobars are included in this figure. The peak point has the coordinates $(x,y) = (0, 0.951625)$, with surrounding crests located at $(\pm 6.22725, 0.46935755)$, $(\pm 12.566, 0.3145638)$. Between these crests, there are two sets of troughs with local minimum values for the elevation, being located at $(\pm 3.1125, -0.25686088)$ and $(9.3860, -0.20652876)$.

$k = 0.5$. This value is slightly above the minimum admissible value for k, when we require a periodic and continuous free surface, not intersecting the lower boundary $\tilde{y} = -k$. The reference level $\tilde{y} = 0$ is chosen according to linear theory. The reference level is not the undisturbed water level for a standing wave of finite amplitude since the focus is on displaying and comparing a family of surface shapes.

Prescribed by Eq. (49), Figure 10 shows peaked surface shapes $\tilde{\eta}(\tilde{x},k)$ displayed as a one-parameter family of shapes depending on the parameter k, ranging from 0.5 to infinity. Moreover, two length scales are illustrated in the figure. The first one is the horizontal length scale 2π for the wavelength, and the second one a vertical length scale k. Rescaling of the coordinates makes the parameter k reappear as a depth instead of its original definition as a wavenumber. Represented are only the two cases $k = 0.5$ and $k \to \infty$, since the varia-

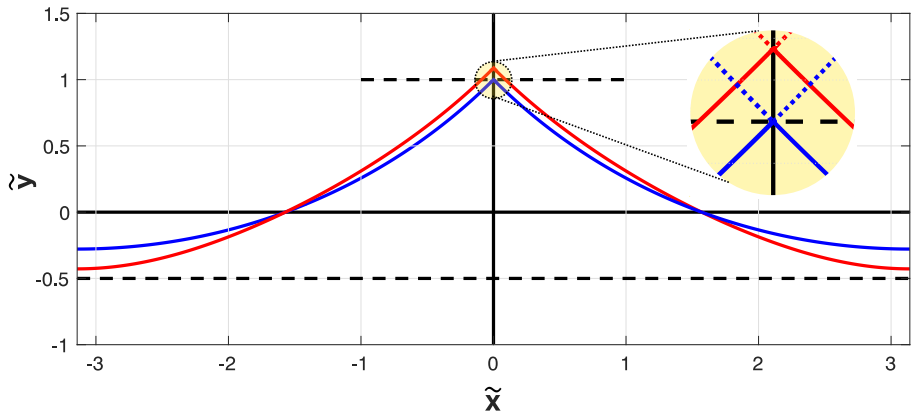

FIG. 10. Plots of two members of the rescaled family of peaked periodic surface contours at uniform depth, based on a single Fourier component $\tilde{\eta}(\tilde{x},k)$, where $-\pi<\tilde{x}<\pi$ shows one wavelength. Blue line represents the deep-water limit where $k\to\infty$, with amplitude $A_1=-0.3678796$ and surface peak at $(\tilde{x},\tilde{y})=(0,1)$. Red line represents the wavenumber $k=0.5$, with amplitude $A_1=-0.853621$ where its associated bottom (dashed) is located at $\tilde{y}=-k=-0.5$.

tion of shapes within this family is quite small, apart from the thinning of the layer near the bottom $\tilde{y}=-k$ as k is reduced. The position of the peak does not vary much with k, confer the magnified marked circle. The lowest peak position is $\tilde{\eta}(0,\infty)=1$.

Figure 10 does not give an exhaustive picture of possible peaked surface shapes at a constant depth. At least two length scales exist, which implies that we cannot in general limit the Fourier solution to one term only, which is an underlying restriction in Figure 10. Admittedly there may be more than two length scales for the highest standing wave at a uniform depth. Therefore it is no surprise that the literature does not offer any consensus concerning the shape of the highest standing periodic wave for a given average depth.

V. FURTHER DISCUSSIONS AND CONCLUSIONS

In their seminal theoretical work for standing waves, Penney & Price[6] claimed that the highest wave surface has a right-angle peak. The experimental results by Taylor[4] supported Penney & Price[6] in their sketched stagnant wave with a right-angle peak, to fall freely under gravity. However, Taylor[4] did not accept the arguments for the right-angle peak from Penney & Price[6], as he remarked that any peak angle could be a valid initial state released from rest. Taylor rightfully hinted that a strictly time-periodic flow cannot produce a peaked surface.

The peaked shape of the highest periodic standing wave avoids artificial undulations when the acceleration potential has only one single Fourier term in the horizontal direction, contrasting the truncated solution by Penney & Price[6], which we highlight in Figure 8. Chen *et. al.*[23] elaborated a Lagrangian description to get a smooth stagnant surface. Their type of theory cannot avoid mass defects, also having to cope with false inflection points and an overshoot around the surface peak.

By the Lambert W function, we have derived the analytical formula $H/L=[W(e^{-1})-W(-e^{-1})]/(2\pi)$, equal to 0.20347 with five digits, which is the result by Grant[7] with improved accuracy. Tsai & Jeng[13] reported a value $H/L=0.2040$ very close to Grant's prediction[7]. The value $H/L=0.1974$ was predicted both by Mercer & Roberts[25] and Wilkening[21]. Furthermore, Okamura[9] derived $H/L=0.1996$ for the relative wave height of the highest standing deep-water wave.

With a chosen quasi-periodicity to create different neighboring crest heights, we found a local peak height to wavelength ratio equal to $H/L=0.194$. This number fits in with the established values around 0.2. We have thereby shown that the relative peak height is robust with respect to deviations from spatial periodicity.

Our minimalist theory for the instantaneous peaked shape of a single Fourier component coincides with the work by Grant[7]. He used a Stokes expansion and performed a one-term truncation horizontally, with an unnecessary series expansion for the dynamic condition in the vertical direction. It had no consequences with respect to numerical accuracy, but made Grant's good work less accessible.

Most work on nonlinear standing waves is based on periodicity in time, with extensions to stability analysis[25,26]. Saffman & Yuen[18] pioneered the modern approach of a fully nonlinear free-surface simulation, generating standing deep-water waves by a sinusoidal pressure of finite duration, applied on an initially flat surface. The waves that were generated failed to be strictly time-periodic, becoming steeper and reach higher elevations than time-periodic waves.

The initial forcing of a standing wave from a flat sur-

face was modeled with high accuracy by Longuet-Higgins & Dommermuth[16]. We share their basic assumption of only one length scale for the initial flow, which is the wavelength. While we picked the highest standing wave as a state of pure acceleration with a sharp peak, these authors confronted the great challenge of picking the highest wave with full periodicity in time. They determined a maximal initial amplitude for the forced flow to be almost periodic in time.

The study of impulsively forcing of a nonlinear Cauchy-Poisson problem[16] is a more causal physical approach than a conventional stability analysis. In spite of this excellent work, it is not yet settled whether a strict amplitude threshold exists for exactly periodic standing waves with full nonlinearity. The simulations by Longuet-Higgins & Dommermuth[16] did not repeat the initially flat surface exactly after one period, a finding that they linked to Penney & Price[6]. An irreversible hysteresis loop emerged for the steepest slope angle, evolving differently during the second half oscillation period compared with the first half period of oscillation. The steepest slope angle of 32° reported in these simulations[16] is in excellent agreement with a handpicked member of our one-parameter family of smooth surface shapes, where the acceleration amplitude is $A = 0.967A_{max}$ with A_{max} defined as the maximum possible value representing the peaked surface.

A challenge for future work is to perform fully nonlinear simulations of smooth free surface shapes released from rest, belonging to in the amplitude range $0.967A_{max} < A < A_{max}$ beyond the reported simulations[16]. Recently, Aurther *et. al.*[27] have developed relevant tools for mathematical modeling of free surface evolution at the edge of peak formation. The sharp peak itself is mathematically troublesome as an initial shape, see Constantin[28].

Large-amplitude standing waves on uniform depth are richer phenomena than the classical deep-water case discussed here. The oscillation frequency as a function of the depth and wave steepness has been studied by Vanden-Broeck & Schwartz[20], Tsai & Jeng[13] and others. With finite depth, any stagnant free-surface acceleration flow will have more than one length scale. In the absence of a single length scale, there is no longer a unique stagnant standing wave. We have exemplified a family of finite-depth solutions with two length scales and a peaked surface.

A general picture of physical length scales is emerging for peaked stagnant water waves with full nonlinearity. (i) The single stagnant wave peak at infinite depth is the only case with no physical length scale. (ii) The spatially periodic standing peaked wave at infinite depth has only one length scale, which is its wavelength. (iii) The periodic standing peaked wave with a horizontal bottom allows several length scales. Our one-parameter family with two length scales does not pretend to cover all configurations.

Compared with free modes of oscillation with finite depth, a privilege of infinite depth is that all higher spatial modes are also higher modes in frequency since the linearized dispersion relation gives a wave number proportional to the square of the frequency. This synchronization of the higher modes makes exact periodicity in time much more plausible for infinite depth than for finite depth, illustrated by the pioneering work by Penney & Price[6]. These authors raised doubts on whether a strictly periodic standing wave exists at high wave steepness, to be supported much later by Longuet-Higgins & Dommermuth[16].

Our single length scale postulate leads to a one-term Fourier component obeying the exact dynamic condition for the stagnant highest standing deep-water wave with periodic surface peaks. On the contrary, Wilkening[21] discovered a richness of small-scale phenomena by numerical simulations, but he gave no causal explanation or dimensional analysis. Wilkening[21] pretended to abolish the self-similarity of the surface peak advocated by Grant[7] by computing much richer structures around the peak. In response, we support Grant Grant[7] by maintaining our postulate of a single length scale, as we see no physical cause for the emergence of a second length scale.

Appendix A gives a proof for the right angle peak of the highest wave released from rest under gravity, consistent with the theory by Grant[7]. We introduce the complex function $\chi(z) = \Phi(z) - z$ for describing the surface peak. The real part of $\chi(z)$ is zero along the free surface, and the peak point is defined by $d\chi/dz = 0$. The peak angle is decided by the leading term in the local Taylor series around the peak point. With a leading term of order N, the peak angle becomes π/N. Under the regular constraints for a released free surface, this Taylor series should have a quadratic term as its leading order, implying a peak angle of $\pi/2$. In Appendix A we show that this the case for our single-term Fourier solution for a periodic standing deep-water wave.

DATA AVAILABILITY

The data that support the findings of this study are available from the corresponding author upon reasonable request.

REFERENCES

[1]G. G. Stokes, "Supplement to a paper on the theory of oscillatory waves," Math. Phys. Papers **1**, 14 (1880).
[2]J. H. Michell, "The highest waves in water," The Lond. Edinb. Dubl. Phil. Mag. & J. Science **36**, 430–437 (1893).
[3]L. W. Schwartz and J. D. Fenton, "Strongly nonlinear waves," Ann. Rev. Fluid Mech. **14**, 39–60 (1982).
[4]G. I. Taylor, "An experimental study of standing waves," Proc. R. Soc. Lond. Ser. A **218**, 44–59 (1953).
[5]J. W. Strutt, "Deep water waves, progressive or stationary, to the third order of approximation," Proc. R. Soc. Lond. Ser. A **91**, 345–353 (1915).
[6]W. G. Penney and A. T. Price, "Some gravity wave problem in the motion of perfect liquids, part ii, finite periodic stationary gravity waves in a perfect liquid," Phil. Trans. A **244**, 255–284 (1952).
[7]M. A. Grant, "Standing Stokes waves of maximum height," J. Fluid Mech. **60**, 593–604 (1973).
[8]M. Okamura, "On the enclosed crest angle of the limiting profile of standing waves," Wave Motion **28**, 79–87 (1998).
[9]M. Okamura, "Standing gravity waves of large amplitude in deep water," Wave Motion **37**, 173–182 (2003).
[10]M. Okamura, "Almost limiting short-crested gravity waves in deep water," J. Fluid Mech. **646**, 481–503 (2010).
[11]E. Villermaux and Y. Pomeau, "Super free fall," J. Fluid Mech. **642**, 147 (2010).

[12]L. W. Schwartz and A. K. Whitney, "A semi-analytic solution for nonlinear standing waves in deep water," J. Fluid Mech. **107**, 147–171 (1981).
[13]C.-P. Tsai and D.-S. Jeng, "Numerical Fourier solutions of standing waves in finite water depth," Appl. Ocean Research **16**, 185–193 (1994).
[14]C. P. Tsai, D. S. Jeng, and J. R. C. Hsu, "Computations of the almost highest short-crested waves in deep water," Appl. Ocean Research **16**, 317–326 (1994).
[15]M. O. Williams, E. Shlizerman, J. Wilkening, and J. N. Kutz, "The low dimensionality of time-periodic standing waves in water of finite and infinite depth," SIAM J. Appl. Dynamic. Syst. **11**, 1033–1061 (2012).
[16]M. S. Longuet-Higgins and D. G. Dommermuth, "On the breaking of standing waves by falling jets," Phys. Fluids **13**, 1652–1659 (2001).
[17]L. Q. Spielvogel, "Single-wave run-up on sloping beaches," Journal of Fluid Mechanics **74**, 685–694 (1976).
[18]P. G. Saffman and H. C. Yuen, "A note on numerical computations of large amplitude standing waves," J. Fluid Mech. **95**, 707–715 (1979).
[19]I. Tadjbakhsh and J. B. Keller, "Standing surface waves of finite amplitude," J. Fluid Mech. **8**, 442–451 (1960).
[20]J.-M. Vanden-Broeck and L. W. Schwartz, "Numerical calculation of standing waves in water of arbitrary uniform depth," Phys. Fluids **24**, 812–815 (1981).
[21]J. Wilkening, "Breakdown of self-similarity at the crests of large-amplitude standing water waves," Phys. Rev. Lett. **107**, 184501 (2011).
[22]P. M. Jordan, "A note on the Lambert W-function: Applications in the mathematical and physical sciences," Mathematics of Continuous and Discrete Dynamical Systems **618**, 247–264 (2014).
[23]Y.-Y. Chen, H.-C. Hsu, and H.-H. Hwung, "A Lagrangian asymptotic solution for finite-amplitude standing waves," Appl. Math. Comp. **215**, 2891–2900 (2009).
[24]J. Wilkening and X. Zhao, "Spatially quasi-periodic water waves of infinite depth," Journal of Nonlinear Science **31**, 1–43 (2021).
[25]G. N. Mercer and A. J. Roberts, "Standing waves in deep water: Their stability and extreme form," Phys. Fluids **4**, 259–269 (1992).
[26]J. Wilkening, "Harmonic stability of standing water waves," Quart. Appl. Math. **78**, 219–260 (2019).
[27]C. Aurther, R. Granero-Belinchón, S. Shkoller, and J. Wilkening, "Rigorous asymptotic models of water waves," Water Waves **1**, 71–130 (2019).
[28]A. Constantin, "The trajectories of particles in stokes waves," Inventiones mathematicae **166**, 523–535 (2006).
[29]P. A. Tyvand, "Initial stage of the finite-amplitude Cauchy-Poisson problem," Water Waves **2**, 145–168 (2020).
[30]C. Kharif, E. Pelinovsky, and A. Slunyaev, *Rogue waves in the ocean* (Springer Science & Business Media, 2008).

Appendix A: Complex analysis concerning the surface peak

We introduce the complex variable $z = x + iy$, where i is the imaginary unit. The dimensionless dynamic condition is found by putting $g = 1$ in the dimensionless version of Eq. (8). We extend the acceleration potential ϕ analytically by introducing the complex potential $\Phi(z,t)$, where $\phi(x,y,t)$ is its real part. This enables us to extend the dynamic condition analytically at $t = 0$ to be written as

$$\Phi - iz = 0, \;\; z = x + i\eta(x,0), \tag{A1}$$

We introduce a new complex function $\chi = \Phi - iz$. The free surface represents an isoline for the real part of this complex function χ in the vertical x,y plane. These isolines are usually smooth, perpendicular to the corresponding isolines for the imaginary part of the same complex function χ. The highest standing wave has a set of surface peaks $\hat{z}_n$ given by

$$\hat{z}_n = \hat{z}_0 + 2n\pi, \tag{A2}$$

where n is any integer. Two neighboring surface peaks are thus one wavelength $L = 2\pi$ apart, measured in the horizontal direction. The central peak is denoted by $\hat{z}_0$. It is by definition located at the y axis, and $y = 0$ represents the average water level (undisturbed free surface). A sharp surface peak can only exist at an extremal point for the complex potential χ, so we have

$$\left.\frac{d\chi}{dz}\right|_{z=\hat{z}_n} = 0. \tag{A3}$$

Around each extremal point for the complex function $\chi(z)$ we can make a local Taylor expansion

$$\chi = B(z-\hat{z}_n)^2 + O(z-\hat{z}_n)^3, \tag{A4}$$

where B is a complex amplitude. By Eq. (A3) the first-order term in this Taylor series vanishes, together with the trivial zeroth-order term. The peak angle for the surface is determined by the leading order of the Taylor expansion in Eq. (A4).

The theory in the main text is based on the single Fourier component potential $\phi = A\cos(x)e^y$, which provides an explicit expression for $\chi(z)$

$$\chi = \Phi - iz = Ae^{-iz} - iz, \tag{A5}$$

with a real amplitude A to ensure that the flow that it represents is periodic in the x direction. The Taylor expansion in Eq. (A4) for χ has the second derivative

$$\left.\frac{d^2\chi}{dz^2}\right|_{\hat{z}_0} = \frac{d^2\Phi}{dz^2} = -\Phi = -iz = -i\hat{z}_0 = \hat{y}_0. \tag{A6}$$

Here we inserted the deep-water Fourier component potential in Eq. (A5), and evaluated it at the central peak point $z = \hat{z}_0 = i\hat{y}_0$. By Eq. (A4) we have

$$\left.\frac{d^2\chi}{dz^2}\right|_{\hat{z}_0} = 2B = \hat{y}_0 > 0, \tag{A7}$$

since the central peak point has a positive elevation $\hat{y}_0$. Thus the highest standing wave represents a local quadratic function near its peak, with nonzero amplitude B. From the complex analysis, we know that a quadratic function z^2 has its isolines meeting at a right angle in the origin, both for its real part (the free surface) and its imaginary part. This completes our proof that the highest standing wave has a right-angle peak. The symmetric potential ϕ around the peak implies that two slope angles $\pm\pi/4$ meet in this peak point.

Our proof for the right-angle peak depends on $d^2\chi/dz^2 \neq 0$ at the peak. This constraint is met by our single-term Fourier solution in Eq. (A5) for the acceleration potential $\Phi = \chi - z$, but it is admittedly satisfied for many other acceleration potentials. Thus the right-angle peak is a result that has broader validity and does not depend on our single length scale postulate. On the other hand, we proved the right-angle peak with our single-term Fourier solution to verify that this peak angle is consistent with our postulate of a single length scale.

Grant[7] performed a more complicated proof for the right-angle surface peak. He allowed a singularity at the peak, even though his leading-order solution had no singularity. Our simple analysis exposes a complex function with quadratic behavior around each local surface peak, without local singularities.

Appendix B: On the highest non-breaking rogue wave

This appendix will relate the highest spatially-periodic standing wave in the main text to isolated wave peaks without periodicity. A single stagnant peaked wave at infinite depth does not have a physical length scale. It has to set its own length scale as its starts to flow under gravity, and by doing so, it defines a similarity solution. A physical length scale needs a cause to come into existence, and a similarity solution emerges in the absence of a cause. Any local surface heap released from rest is an initial legal state if it satisfies the asymptotic far-field condition

$$\eta(x,0) \to 0 \text{ as } x \to \pm\infty, \tag{B1}$$

with finite surface slope $\partial\eta(x,0)/\partial x$ everywhere.

Physical candidates for the highest stagnant single wave with a sharp peak can only be found among flow potentials that do not have length scales of their own, which is the basic assumption to be pursued in this appendix. The highest stagnant peaked rogue wave in deep water should have no physical length scale, whereby it becomes a similarity solution for free-surface flow released from rest. The acceleration potential for this initial gravitational flow is the real part of a complex potential $\Phi(z,0)$ where $z = x + iy$. This complex acceleration potential has its singularities outside the fluid domain. A candidate for the single peak acceleration potential can only have one single multipole located in one single point, chosen as $z = Hi$. Only one singularity in one singular point is legal, for avoiding that singularities have their own length scale. H can be arbitrary but positive ($H > 0$) in order to satisfy the far-field condition in Eq. (B1).

A stagnant standing deep-water wave with one single peak is a rogue wave, according to the classification by Kharif *et al*.[30]. The alternative notion of freak wave indicates that the highest rogue waves in the open sea are breaking waves. However, only a non-breaking rogue wave may achieve a state of rest where the entire energy is potential energy in the gravity field, which is admittedly a highly idealized state. A completely motionless state with a sharp peak must be regarded as a theoretical upper limit for a single rogue wave. It is much less realistic than the corresponding model of periodic waves by Grant[7]. We will now investigate the highest non-breaking rogue wave generated by a single multipole, which we place at a height H above the undisturbed free surface.

The source potential $\Phi = \log(z - Hi)$ is not a legal candidate for the acceleration potential because it gives a nonzero mass flux at infinite depth. The simplest acceleration potential to be considered is therefore the vertical dipole potential

$$\phi(x,y,0) = A\frac{y-H}{x^2+(y-H)^2}. \tag{B2}$$

It represents the derivative of the source potential, and is here written as a flow potential in real form. We choose the unit height $H = 1$ for computation of the free-surface shape, see Figure 11 (a). This initial free surface is given by inserting the acceleration potential in the dynamic condition of Eq. (20), and the surface level goes to zero as $|x| \to \infty$. We note that the surface elevation goes very slowly to zero in the far-field for the single dipole. This is a peculiarity due to infinite depth, while a horizontal bottom would imply a quadrupole far-field behavior from a single dipole plus its image dipole located below the horizontal bottom. For achieving a realistic far-field with infinite depth, we therefore need to discard the dipole and choose the next order multipole, which is the quadrupole.

In Figure 11 (b), we show the initial free surface due to the symmetric quadrupole acceleration potential

$$\phi(x,y,0) = A\frac{x^2-(y-H)^2}{(x^2+(y-H)^2)^2}. \tag{B3}$$

Again we choose $H = 1$ for this plot, where the decay of the surface elevation towards infinity is satisfactory. A sign change occurs at $|x| = H$, where the surface elevation is positive inside the domain $-H < x < H$ and negative outside it.

The symmetric surface shape is of primary interest, but we also want to see an asymmetric case that sets its own length scale. If we rotate this quadrupole potential an angle $\pi/4$, the resulting antisymmetric potential has the form

$$\phi(x,y,0) = A\frac{x(y-H)}{(x^2+(y-H)^2)^2}, \tag{B4}$$

and the resulting free-surface shape has the strongest asymmetry possible generated by a single quadrupole. The resulting surface shape is plotted in Figure 11 (c). Because of the antisymmetry of the potential around $x = 0$, the surface elevation is zero at this point, while the surface shape is not at all antisymmetric around $x = 0$. This has to do with the distance from each surface point to the quadrupole singularity, as the nonlinearity at the free surface tends to get stronger the shorter the distance from the singularity. In Figure 11, we have extended the surface contour outside the fluid domain, as a reminder that these mathematical curves are closed loops intersecting the singular point $z = iH$.

Our above considerations have led us to the symmetric quadrupole as the best candidate for a peaked stagnant rogue wave in the open sea. Since it has no physical length scale, no estimate of its highest possible physical wave height comes from this peaked surface shape. An isolated rogue-wave peak may be released as a Cauchy-Poisson problem in order to link it to the physical wavelengths of oscillatory waves.

In Figure 12 we compare this peaked rogue wave with the corresponding stagnant wave peak of periodic waves studied in the main text. We must normalize these waves properly in order to make them directly comparable with one another. This is done by requiring that the surface peak has a unit height in both cases.

(i) For the periodic wave, the definition of the zero wave height for the periodic wave is taken to be the wave trough, which means to upscale the value of $H/L = 0.20347$ (Grant's result) to $H = 1$, magnifying the length unit in Figure 4 by a factor of $1/0.20347 = 4.9147 = 2 \times 2.4573$.

(ii) For the single wave peak, the natural level of zero wave height is the far-field level $y = 0$, which is used already in Figure 11 (b) but resulted in a peak height of 0.33205, with $H = 1$ referring to the quadrupole position. We, therefore, magnify

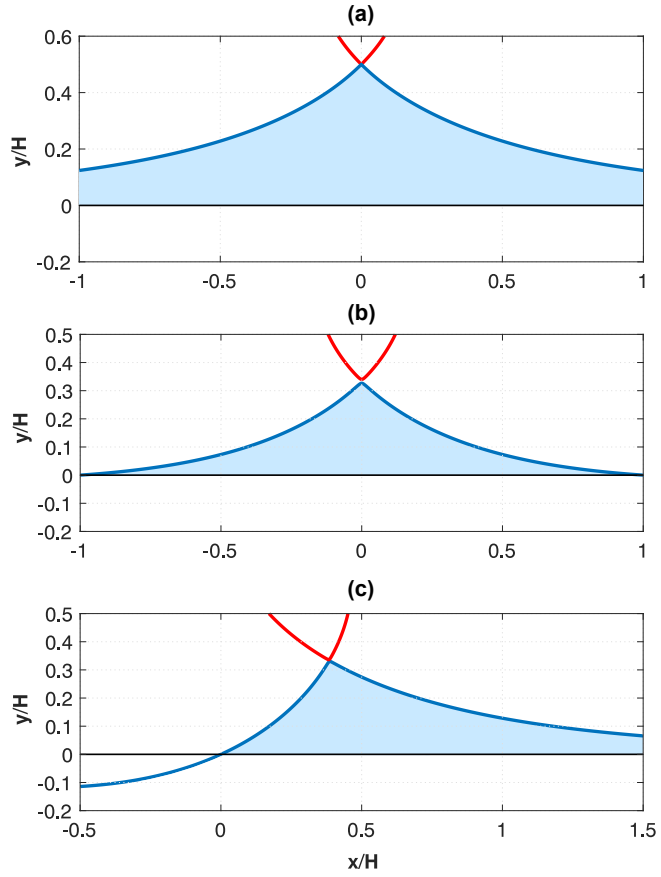

FIG. 11. Acceleration potentials with one singularity point in $(0,1)$. The initial peaked free-surface shapes $\eta(x,0)$ are shown, together with the undisturbed free surface $y=0$. **a)** Vertical dipole potential: $\phi(x,y,0)=A(y-1)/(x^2+(y-1)^2)$, where $A=0.25$. **b)** Symmetric quadrupole potential: $\phi(x,y,0)=A(x^2-(y-1)^2)/(x^2+(y-1)^2)^2$, where $A=0.1481$. The peak point is (0,0.33205). **c)** Antisymmetric quadrupole potential: $\phi(x,y,0)=Ax(y-1)/(x^2+(y-1)^2)^2$, where $A=0.45615$.

the length unit in Figure 11 (b) by a factor of 1/0.33205 = 3.0116, so that the length unit H no longer represents the location of the mathematical singularity, but instead it represents the height of the peak above the undisturbed level at infinity.

In Figure 12 we have achieved a visual comparison between one wavelength $(-2.4573 < x/H < 2.4573)$ for the peaked periodic wave and the inner region of positive elevation $-3.0116 < x/H < 3.0116$ for the peaked isolated wave. These two rescaled solutions now share the local quadratic flow potential around their common peak, which we observe from the figure. The two surface contours start to deviate from one another, where the local Taylor series for both these solutions involve more than two terms. The caption of Figure 12 includes numerical calculations of the areas above $y=0$ for the periodic wave and the single isolated wave, showing that the latter area is about 20 per cent greater than the area for the periodic wave (with blue color).

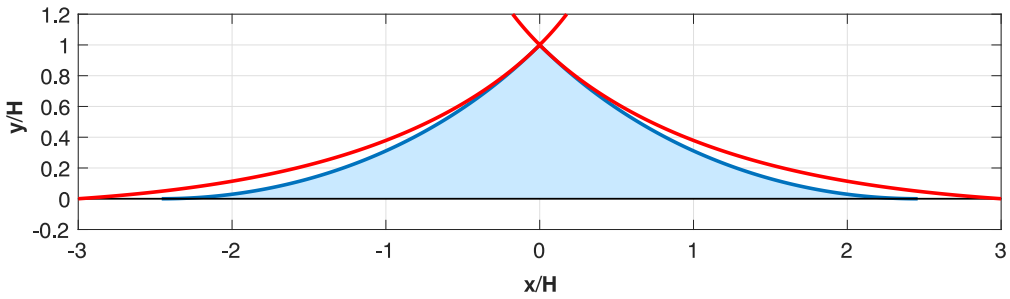

FIG. 12. The periodic highest wave from the main text is rescaled with unit wave height. The dimensionless area above the undisturbed surface $y = 0$ is 1.518, with blue color. The height is 1 with one wavelength width $2\pi/1.2785$, implying that one wavelength is contained within the domain $-2.4572 < x < 2.4572$. The red curve shows the surface shape of a single-peak stagnant rogue wave from one symmetric quadrupole, with singular point at $y = H = 1.2785$, and with unit height of the peak. Its dimensionless area is 1.83748968, within the domain of positive surface elevation $-3 < 3x < 3$.